CrystEngComm

Cite this: *CrystEngComm*, 2012, **14**, 8606–8614

www.rsc.org/crystengcomm

PAPER

Synthesis and crystal structure of three new cadmium tartrates with open frameworks†

Paula Vera-Cruz,[a] Rubén A. Toscano,[b] Jorge Balmaseda,*[a] Mario Basterrechea,[cd] Netzahualcoyotl Niño[a] and Luis Felipe del Castillo*[a]

Received 16th August 2012, Accepted 3rd October 2012
DOI: 10.1039/c2ce26312b

Four metal–organic coordination polymers: $\{[Cd_3(C_4H_4O_6)_3(H_2O)]\cdot H_2O\}_n$ **I**, $\{[Cd_3(C_4H_3O_6)_2(H_2O)_2]\cdot 5.5H_2O\}_n$ **II**, $\{[Cd_2(C_4H_4O_6)_2(H_2O)]\cdot 3H_2O\}_n$ **III**, and $[Cd(C_4H_4O_6)]_n$ **IV** were obtained under hydrothermal conditions and characterized by IR spectroscopy and single crystal X-ray diffraction. The structural analysis reveals that compounds **I**–**III** exhibit new 3D open frameworks filled with water molecules, which according to thermogravimetric analysis evolve at temperatures significantly lower than onset temperatures for decomposition. Compound **I** exhibits an 8-c net; uninodal net (eci net) with Schläfli symbol $\{3^6\cdot4^{12}\cdot5^{10}\}$, where Cd atoms are connected by μ_4,κ^6-mode and μ_4,κ^5-mode tartrate ligands. Compound **II** is a rare example of a tartrate trianion complex formed by μ_5,κ^6-mode ligands creating a (6,3)-connected net with Schläfli symbol $(4\cdot6^2)_2(4^2\cdot6^{10}\cdot8^3)$. Compound **III** exhibits a 3,3,4,4-connected, 4-nodal net with Schläfli symbol $\{4\cdot8^2\}\{4\cdot8^4\cdot10\}$, built up by dimers of two octahedral Cd atoms linked by μ_4,κ^6-mode and μ_3,κ^5-mode tartrate ligands. Compound **IV** was previously reported although being obtained under different synthetic conditions and can be described as a 5,5,11-connected, 3-nodal net with the Schläfli symbol of $\{3^2\cdot4^6\cdot5^2\}2\{3^4\cdot4^{14}\cdot5^{16}\cdot6^{18}\cdot7^2\cdot8\}\{3^4\cdot4^3\cdot5^2\cdot6\}$. None of the compounds reported here are topologically related, evidencing the versatility of the tartrate ligand for the framework formation of coordination polymers.

Introduction

Compounds with tartrate anions have been studied since the tenth century, when the Arabic alchemist Geber isolated tartaric acid from tartar.[1] The interest in these compounds is motivated by the fact that the tartrate anion can exhibit a variety of coordination abilities, where both hydroxyl and carboxylic groups can make various bridges between metal atoms.[2–4] In addition, one or both hydroxyl groups can be deprotonated,[5–8] allowing them to coordinate to more than one metal atom and leading to a wider range of binding modes. The aforementioned properties make the tartrate ligand a good candidate for designing new flexible and open metal–organic frameworks.[8–11] These frameworks may exhibit an exceptional flexibility and stimulus-responsive behavior, reacting to changes in temperature, pressure, and adsorption of guest molecules by undergoing structural transformations.[12–15] Such materials have promising applications as sensors and actuators, as well as in adsorptive retention and separation.[16–21] However, it is remarkable that a small number of studies about open frameworks based on the tartrate ligand can be found in the literature.

The Cd(II) atom, with d^{10} configuration, exhibits a wide variety of coordination geometries and modes that can induce versatile structural topologies.[22] So far, only four structures of Cd L-tartrate have been reported, all with different dimensionalities, levels of hydration and porosity.[2,23–25] Moreover, Torres *et al.*[26] reported the dependence of the crystal structure of $[Cd_2(C_4H_4O_6)_2(H_2O)]\cdot 3H_2O$[24] with temperature, identifying phase transitions as the structure is heated or cooled. This finding points to the possibility of the existence of a larger number of crystalline structures of cadmium tartrate.

This work is an effort to expand the known universe of cadmium tartrates. We report three new phases: $\{[Cd_3(C_4H_4O_6)_3(H_2O)]\cdot H_2O\}_n$ **I**, $\{[Cd_3(C_4H_3O_6)_2(H_2O)_2]\cdot 5.5H_2O\}_n$ **II**, and a polymorph of $\{[Cd_2(C_4H_4O_6)_2(H_2O)]\cdot 3H_2O\}_n$ **III**; and reproduce a compound previously reported $[Cd(C_4H_4O_6)]_n$ **IV**[2a,2b] through different synthetic routes. The four compounds were obtained under hydrothermal conditions using the same reactants. They

[a]*Departamento de Polímeros, Instituto de Investigaciones en Materiales, Universidad Nacional Autónoma de México, Circuito Exterior, Ciudad Universitaria, México D.F. C.P. 04510, Mexico. E-mail: lfelipe@unam.mx; balmaseda@iim.unam.mx; Tel: +52 5556224723*
[b]*Instituto de Química, Universidad Nacional Autónoma de México, Circuito Exterior, Ciudad Universitaria, México D.F. C.P. 04510, Mexico*
[c]*Facultad de Química, Universidad de La Habana, Zapata y G, Vedado, La Habana, Cuba*
[d]*Instituto de Ciencia y Tecnología de Materiales, Universidad de La Habana, Zapata y G, Vedado, La Habana, Cuba*

† Electronic supplementary information (ESI) available: Selected bond distances and angles, and selected hydrogen bond lengths and angles. CCDC 872860–872862. For ESI and crystallographic data in CIF or other electronic format see DOI: 10.1039/c2ce26312b

exhibit a diversity of structures with varying connectivity, chemical composition, porosity, and level of hydration.

Experimental section

Materials and general methods

Infrared spectra (4000–400 cm^{-1}) were obtained using a Nicolet FT-IR 6700 spectrometer. The mode of acquisition of the spectra was by means of the ATR or transmission technique.

Thermogravimetric analyses were carried out using a TA Instruments high resolution (Hi-Res^{TM}) thermogravimetric analyzer, TGA 2950. The mass loss profiles of the studied samples were analyzed using the instrument control software Universal Analysis 2000 v4.4A. The heating rate was dynamically controlled from 0.001 °C min^{-1} to 5 °C min^{-1} (instrumental resolution = 5) in air atmosphere with a purge rate of 62.5 mL min^{-1}.

The dehydration–hydration cycles were carried out using the DVS-Advantage instrument (Surface Measurement Systems, London, UK). This instrument measures the uptake and loss of water vapor gravimetrically using a recording ultra-microbalance with a mass resolution of ±0.1 μg. The vapor partial pressure (±1.0%) around the sample was controlled by mixing saturated and extra dry air streams using electronic mass flow controllers. The air used as carrier gas was supplied by INFRA, S.A. de C.V. The instrument temperature was maintained at 20.0 ± 0.1 °C. Approximately 55 mg of the sample was placed into the sample pan, which hung in the balance. It was then heated at 1 °C min^{-1} to 100 °C, kept at 100 °C for one hour, and cooled back to 20 °C at 1 °C min^{-1}. All processes were carried out in a 100 sccm stream of extra dry air. The sample was then hydrated in a 100 sccm stream of air at 95% relative humidity for twenty hours. The dehydration–hydration cycle was carried out three times.

X-ray powder diffraction patterns were obtained with a Bruker-D8 Advance diffractometer equipped with a Cu-tube, a primary germanium monochromator and a Vantec-1 detector.

Synthesis

All reactions were carried out under hydrothermal conditions in 85 ml Teflon-lined stainless steel autoclaves. An exploratory 3^3 factorial experiment was implemented where: temperature, heating time and molar ratio factor levels were: 75 °C, 90 °C, and 120 °C; 24 h, 72 h, and 120 h; and 3 : 5, 5 : 5, and 5 : 3; respectively. In all cases, a 10 mL aqueous solution of cadmium acetate dihydrate ($Cd(C_2H_3O_2)_2{\cdot}2H_2O$, Sigma-Aldrich ⩾97%) was added to a stirred 10 mL aqueous solution of potassium L-tartrate dibasic hemihydrate ($K_2(C_4H_4O_6){\cdot}0.5H_2O$, Riedel-deHaën ⩾98%). Once the heating time was completed, the reactions were gradually cooled to room temperature, and the precipitates were washed with water and dried in air.

The X-ray powder diffraction patterns revealed that in all cases compounds **I**–**IV** were obtained either pure or as a mixture. Table 1 summarizes the conditions where compounds **I** and **IV** were obtained pure and compounds **II** and **III** were obtained as highly predominant phases (see PXRD in Fig. S1–S4, ESI†); phase purity and predominance of the products was confirmed by comparison of the experimental powder pattern *versus* that calculated on the basis of the structures reported here. In all cases, pure single crystals of the studied compounds were removed by manual separation for single crystal X-ray diffraction, IR, TG and dehydration–hydration studies.

Table 1 Synthetic conditions and crystal morphology for **I–IV**

	Concentration[a]				
	KTa, M	CdAc, M	Temp, °C	Heating time, h	Crystal color and shape
I	0.5	0.3	75	24	White needle
II	0.3	0.5	90	120	Yellow prism
III	0.5	0.3	120	72	White prism
IV	0.5	0.5	120	72	White prism

[a] KTa: $K_2(C_4H_4O_6){\cdot}0.5H_2O$, CdAc: $Cd(C_2H_3O_2)_2{\cdot}2H_2O$.

X-ray crystallography

Suitable crystals of compounds **I**–**IV** were mounted on a Bruker Smart APEX II CCD diffractometer equipped with graphite-monochromated Mo Kα radiation (λ = 0.71073 Å). Data collection was carried out by using the ω scan technique at room temperature, except for compound **II** which was collected at low temperature in an attempt to minimize the thermal motion of the water molecules. Absorption corrections were based on symmetry equivalent reflections using the SADABS program.[27] The structures of **I**, **II** and **III** were solved by direct methods with SHELXS-97 and followed by successive Fourier and difference Fourier syntheses and refined by full-matrix least-squares on F^2.[28] All non-hydrogen atoms were refined with anisotropic displacement parameters. The hydrogen atoms attached to C atoms were placed in calculated positions and refined isotropically using a riding model with an U_{iso}(H) equivalent to 1.2 times of U_{eq}(C). For those bound to water molecules and hydroxyl groups, were initially located in a difference Fourier map and included in the final refinement by use of geometrical constraints or restraints with the O–H distances being fixed at 0.85 Å, and U_{iso}(H) equivalent to 1.5 times of U_{eq}(O). Crystal data as well as details of data collection and refinements for the new complexes are summarized in Table 2. For selected bond distances and angles see Table S1, ESI;† for selected hydrogen bond lengths and angles see Table S2, ESI.†

Having found the unit cell parameter for **IV**‡, a survey on the Cambridge Structural Database§ indicated that this compound had been previously reported twice, with CCDC refcodes: UPIXUN[2a] (dehydrated form) and XUBMEN[2b] (partially hydrated).

Estimation of solvent accessible voids in the crystal structures was calculated using the CALC VOID[29] function of PLATON[30] (update 03/Jul/2012) with a gridstep of 0.10 Å and taking valid grid points at least 1.20 Å from nearest van der Waals surface. The lattice water molecules were manually removed from the CIF file of each structure before carrying out the calculations.

Results and discussion

Description of the crystal structures

The X-ray diffraction analysis reveals that compounds **I**–**IV** exhibit very different molecular structures; therefore, their

‡ Crystal data for **IV**: orthorhombic, space group $C222_1$, a = 10.7901, b = 11.1995, c = 30.5880 Å, V = 3696.3 $Å^3$, Z = 24.
§ CSD version 5.33 (November 2011) & updates (Feb, May 2012).

Table 2 Crystal data and structural refinement parameters for **I–III**

	I	II	III
Formula (Sum)	$C_{12}H_{16}Cd_3O_{20}$	$C_{16}H_{42}Cd_6O_{39}$	$C_8H_{16}Cd_2O_{16}$
Formula wt (Sum)	817.45	1532.90	593.01
T, K	298(2)	100(2)	298(2)
Wavelength, Å	0.71073	0.71073	0.71073
Crystal shape	Needle	Prism	Prism
Crystal size, mm	0.07 × 0.12 × 0.49	0.12 × 0.14 × 0.19	0.20 × 0.14 × 0.11
Crystal system	Orthorhombic	Orthorhombic	Monoclinic
Space group	$P2_12_12_1$	$P2_12_12$	$P2_1$
a, Å	6.4001(3)	13.7005(14)	7.6393(8)
b, Å	17.2148(9)	15.6523(16)	11.5121(12)
c, Å	18.6406(9)	9.4417(10)	9.0174(10)
α,°	90	90	90
β,°	90	90	99.3050(10)
γ,°	90	90	90
V, Å^3	2053.76(18)	2024.7(4)	782.59(14)
Z	4	2	2
F(000)	1568	1476	576
D_{calc}, g cm^{-3}	2.644	2.514	2.517
Absorption coefficient, mm^{-1}	3.182	3.216	2.807
R_{int}	0.0212	0.0540	0.0182
Reflections (collected/unique)	16 295/3729	19 407/5914	6492/2854
Parameters/"observed" reflections	340/3679	315/5447	271/2725
Flack parameter	0.01(2)	0.03(5)	0.02(2)
$R_1{}^a$ [$I > 2\sigma(I)$]	0.0174	0.0431	0.0184
w$R_2{}^b$ [$I > 2\sigma(I)$]	0.0400	0.0935	0.0414
$R_1{}^a$ [all]	0.0177	0.0472	0.0197
w$R_2{}^b$ [all]	0.0402	0.0950	0.0420
Goodness-of-Fit (GOF) on F [$I > 2\sigma(I)$]	1.058	1.054	1.013

^{a} $R_1 = \sum||F_o| - |F_c||/\sum|F_o|$. ^{b} w$R_2 = [\sum w(F_o^2 - F_c^2)/\sum w(F_o^2)^2]^{1/2}$.

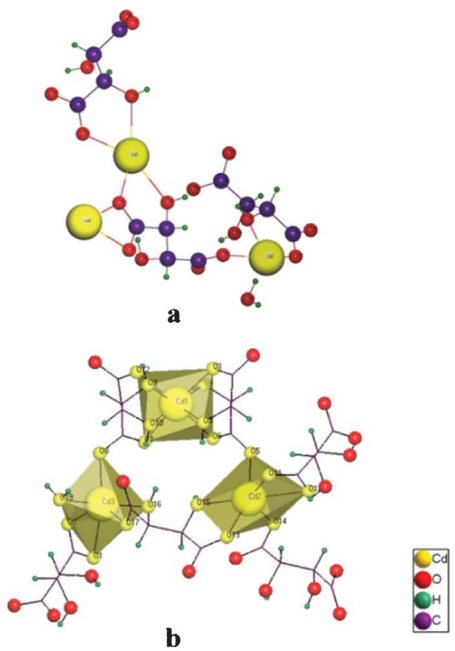

Fig. 1 (a) Asymmetric unit of **I**. (b) Coordination environment of the Cd atoms, represented with yellow polyhedra.

crystal structures are described in detail to represent their frameworks.

{[Cd$_3$(C$_4$H$_4$O$_6$)$_3$(H$_2$O)]·H$_2$O}$_n$ (I). The asymmetric unit of **I** (Fig. 1a) contains three crystallographically independent Cd(II) cations, three tartrate ligands (L1: C1 → C4, O1 → O6; L2: C5 → C8, O7 → O12 and L3: C9 → C12, O13 → O18), one coordinated water molecule (O19), and one lattice water molecule (O20). Tartrate ligands L1 and L2 have the same coordination modes: μ_4,κ^6-mode (bis '1,2-chelation', bidentate carboxylate and monodentate carboxylate in *anti* conformation) (Scheme 1a), while L3 displays the μ_4,κ^5-mode ('1,2-chelation' and bismonodentate carboxylates in *anti* conformation and monodentatehydroyl) (Scheme 1b).

The Cd(1) ion is octa-coordinated, exhibiting a slightly distorted square-antiprismatic environment of oxygen atoms provided by L1 (top) and L2 (bottom) tartrate ligands. The two square faces of the coordination polyhedron are tilted 38.8° to each other and they are quasi-parallel (angle 6.2°). The Cd(2) and Cd(3) ions exhibit distorted octahedral geometries, for atom Cd(2) it is completed by six O atoms from tartrate anions, while for Cd(3) five O atoms come from tartrate anions and one from the coordinated water molecule (Fig. 1b). These trimers are grafted onto the 3D infinite polymer. From a topological[31] perspective, the [Cd$_3$] fragments can be regarded as the network nodes (see Fig. S5, ESI,† for a detailed description); resulting in a final 8-c net; uninodal net (eci net) with the Schläfli symbol of $\{3^6{\cdot}4^{12}{\cdot}5^{10}\}$ (Fig. 2a).

The framework exhibits narrow elliptic channels along the *a* axis, where the coordinated water molecules are situated; these channels are connected to the cavities where the lattice water molecules are located (Fig. 2b). Within these cavities, the lattice water molecules are involved in linear and bifurcated hydrogen bonds with coordinated carboxylic O atoms. In the rest of the hydrogen bonding scheme, all possible hydrogen bonds are formed.

{[Cd$_3$(C$_4$H$_3$O$_6$)$_2$(H$_2$O)$_2$]·5.5H$_2$O}$_n$ (II). Crystal structure analysis reveals that compound **II** is unique in several ways: it is a

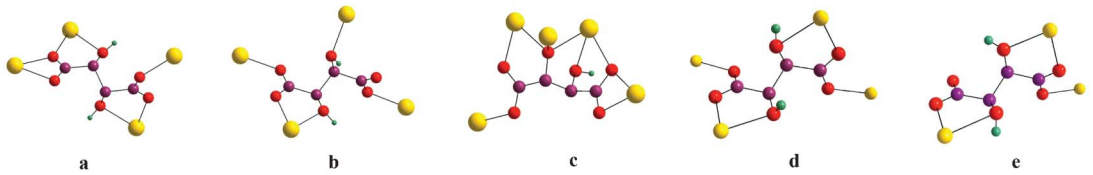

Scheme 1 Binding modes of tartrate ligands: (a) μ_4,κ^6 and (b) μ_4,κ^5 in **I**; (c) μ_5,κ^6 in **II**; (d) μ_4,κ^6 in **III** and **IV**; and (e) μ_3,κ^5 in **III**.

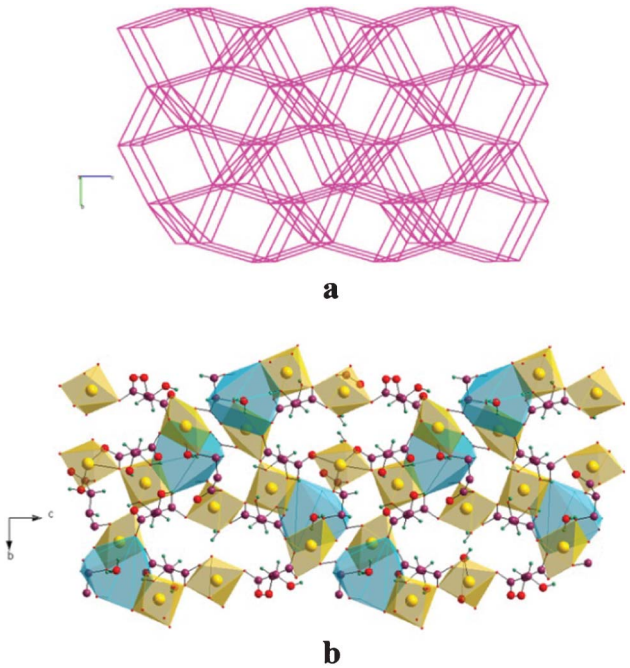

Fig. 2 (a) Schematic representation of the network topology. (b) View of the extended structure of **I** showing the elliptic channels that run along the crystallographic *a* axis, and the cavities containing the lattice water molecules (blue polyhedra).

rare example of a tartrate trianion complex,[5,32] it comprises the structure of an oxygen bridged heterocubane cadmium cluster, and, though molecular Cd_4O_4 are known, it possesses an unprecedented 3D polymeric structure of this structural motif. The molecule of **II** lies on a two-fold axis and the asymmetric unit contains three Cd(II) ions, two tartrate tri-anions (L1: C1 → C4, O1 → O6; L2: C5 → C8, O7 → O12), two coordinated water molecules and 5.5 lattice water molecules (Fig. 3).

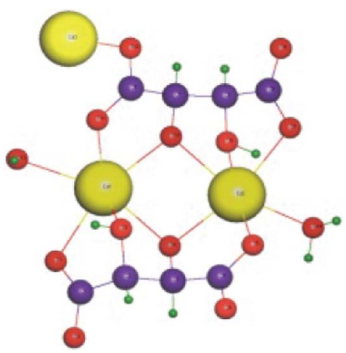

Fig. 3 Asymmetric unit of **II** composed of a tartrate trianion complex (lattice water molecules are omitted for clarity).

Both tartrate ligands have a charge of −3, arising from the deprotonation of one hydroxyl group. This has a profound effect on the structure, with the alkoxy oxygens bridging three Cd atoms, while the OH groups are bound to a single metal ion. The resulting coordination mode of both ligands is a μ_5,κ^6-mode (1,2,3-tris chelate, 1,2 chelate, bidentate carboxylate, monodentate carboxylate in *anti* conformation and monodentate hydroxide) (Scheme 1c).

The molecule has a heterocubane core with hepta-coordinated Cd(1), Cd(2) cations – displaying a capped octahedral coordination – and μ_3-O_{alkoxy} atoms (O4 and O10) occupying alternative vertices (Fig. 4a) linked by octahedral Cd(3) centres (Fig. 4b). Inorganic corrugated layers are formed on the *ab* plane and connected by the tartrate ligands to build a three-dimensional polymer (Fig. 4c).

The network topology can be better represented by considering the Cd_4O_4 heterocubane core (represented by a 6-connected node) and octahedral Cd(3) atom (represented by a 3-connected node). The resulting binodal net is shown in Fig. 5a. Such a (6,3)-connected net can be characterized by the well-known (3,6)-rtl rutile net with Schläfli symbol $(4\cdot6^2)_2(4^2\cdot6^{10}\cdot8^3)$.

In this structure, elliptic channels are formed along the [001] direction with dimensions *ca.* 6.21(1) Å by 7.96(1) Å¶, and they are filled by a cooperative hydrogen bond finite chain (O15 → O19) (Fig. 5b). The remaining uncoordinated water molecule (O20) residing on the a two-fold axis, acts as a bridge – donating and accepting hydrogen atoms from and to the coordinated O13 and O14 water molecules – linking two Cd_4O_4 heterocubane moieties and being encrypted by them. Consequently, compound **II** has an open and potentially porous net with water molecules dispersed throughout the framework.

$\{[Cd_2(C_4H_4O_6)_2(H_2O)]\cdot3H_2O\}_n$ (III). The crystal structure of compound **III** is formed by the $[Cd_2(L\text{-tart})_2(H_2O)]$ dimer acting as a structural repeating unit (Fig. 6a). Structures built up from similar dimeric units are well documented for metal tartrate complexes;[3,4,9,17,33–40] including a polymorph of **III**.[24]

The tartrate ligand L1 has a μ_4,κ^6 coordination mode (bis '1,2-chelation' and bismonodentate carboxylate in *anti* conformation) (Scheme 1d), while L2 displays the μ_3,κ^5-mode (bis '1,2-chelation' and monodentate carboxylate in *anti* conformation) (Scheme 1e). The two metal centers in the dimer display an octahedral coordination showing rhombic distortion, with four short Cd–O distances and two longer Cd–O distances in *cis* orientation, which correspond to the OH groups (O3, O4, O9, and O10).

¶ Pore diameter values were obtained by considering the van der Waals radii of the atoms making up the pores.

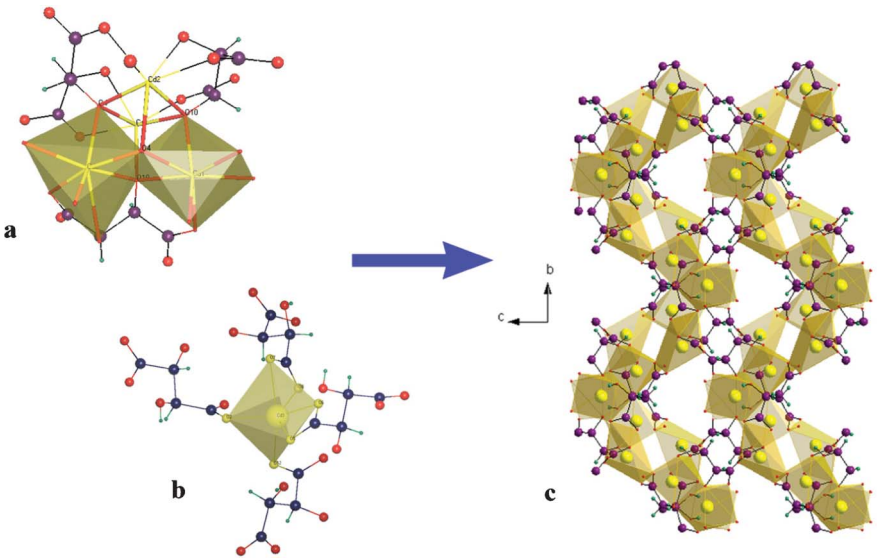

Fig. 4 (a) Heterocubane core formed by Cd1 and Cd2 in compound **II**. (b) Coordination environment of Cd3. (c) View of the resulting inorganic corrugated layers along the *a* axis, lattice water molecules are omitted for clarity.

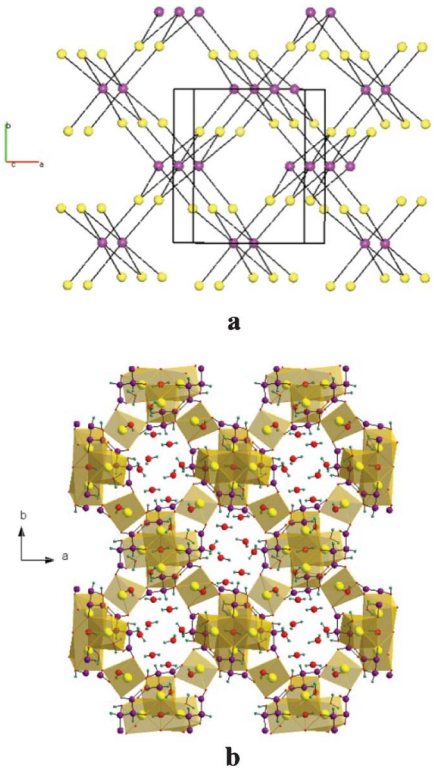

Fig. 5 (a) Schematic representation of the network topology of **II**. (b) View of the elliptic channels formed along the [001] direction.

The extended structure forms polymeric sheets parallel to the *bc* plane (Fig. 6b), connected by the O6 carboxylate atoms and a network of hydrogen bonds involving the water molecules, hydroxyl and carboxylic O atoms (Fig. 6c); creating a porous three-dimensional structure with channels along the *b* and *c* directions (Fig. 7a and 7b). These framework channels intersect to create large cavities containing all the water molecules forming a cooperative hydrogen bond finite chain (O14 → O16). In the hydrogen bonding scheme, all possible hydrogen bonds are formed.

Topologically, compound **III** can be described as a 3,3,4,4-connected, 4-nodal net with the Schläfli symbol of $\{4\cdot8^2\}\{4\cdot8^4\cdot10\}$ (Fig. 7c); where Cd1 and tartrate O1–O6 act as four-connected nodes, Cd2 and tartrate O7–O12 act as three-connected nodes. Examining the TTD database it was found that the same net is observed for the compound *catena*-[(μ^4-L-tartrato)-(μ^3-L-tartrato)-aqua-di-manganese(ii) trihydrate] that is actually the Mn isomorph of **III** and previously reported with CCDC refcodes: TEKDUI[40] (wrong absolute configuration), TEKDUI01[23] and UPIYAU.[2a]

$[Cd(C_4H_4O_6)]_n$ (IV). Compound **IV** has been previously reported twice, in its dehydrated[2a] and partially hydrated[24] forms, although being obtained by different synthetic methods.

According to the description by Lu *et al.*,[2a] the asymmetric unit of **IV** contains four Cd atoms and three tartrate anions, where all tartrate ligands adopt a μ_4,κ^6 coordination mode (Fig. 2d) and all Cd ions adopt a octahedral geometry. Cd(1) and Cd(2) atoms are chelated simultaneously by two equal tartrate ligands through the hydroxyl and carboxylate groups to form a $[Cd_2(L\text{-tart})_2]$ dimer; these dimers are further linked to form a 2D coordination layer. Similarly, Cd(3) and Cd(4) atoms are chelated by tartrate ligands to form dimers that are also linked into another layer. These layers are stacked along the *c* axis, resulting in a 3D anhydrous framework that may accommodate guest water molecules within small channels. Topologically, compound **IV** can be described as a 5,5,11-connected, 3-nodal net (see Fig. S6, ESI,† for a detailed description), with the Schläfli symbol of $\{3^2\cdot4^6\cdot5^2\}2\{3^4\cdot4^{14}\cdot5^{16}\cdot6^{18}\cdot7^2\cdot8\}\{3^4\cdot4^3\cdot5^2\cdot6\}$.

In addition, the topologies for two other reported cadmium tartrates HIXWIU[23,24] and CCDC 791340[25] were calculated (Table S4, ESI†). The analysis of the distribution of the topological types revealed that, besides the similar composition (Cd(II) ions, tartrate ligands and water molecules), all the nets formed posses different topologies, except for the pair:

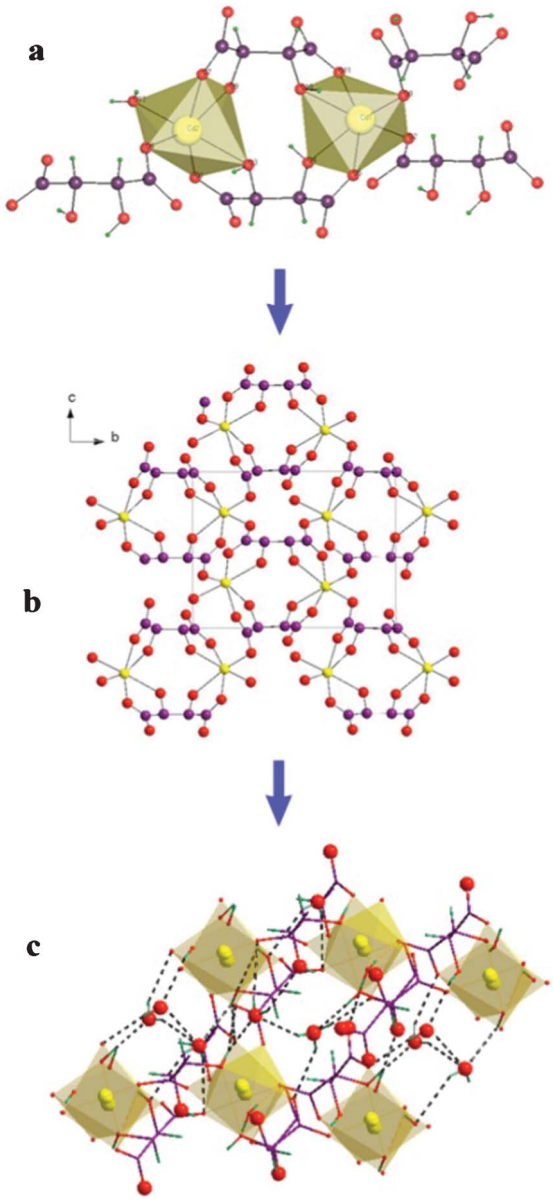

Fig. 6 (a) Dimeric unit building up the asymmetric unit of **III**, lattice water molecules are omitted for clarity. (b) Assembly of the dimers within the sheets. (c) View of the crystal structure along the *b* axis showing the hydrogen-bonding scheme between two sheets. Connecting O6 carboxylate atoms are shown as a ball and stick model.

compound **III** and HIXWIU, precluding any generalization or prediction.

Structural features of the tartrate ligand

In compounds **I**–**IV** the tartrate ligand displays diversiform bridging fashions in the structural assembly (Scheme 1), thanks to its ability to interact through both O atoms in the carboxylate groups as well as both O atoms of the hydroxyl groups. The tartrate anions in compounds **I**, **III** and **IV** have similar μ_3 and μ_4 coordination modes, which vary significantly from the μ_5 coordination modes in compound **II**. It is found that the deprotonation of one hydroxyl group has a profound effect on the binding modes of the ligands, with the alkoxide oxygen bridging three Cd atoms instead of the single Cd bonded to the OH groups.

The bridging variety of the tartrate ligands is further enriched by the different coordination modes adopted by the carboxylate groups of the tartrate ligands. Three coordination modes are found in the four compounds: chelating–bridging tridentate, bridging bidentate and monodentate. The most common mode in all the structures, occurring 14 times, is bridging bidentate, with one Cd shared with other tartrate anions and the other shared with the nearest OH group through a 1,2-chelate ring. There are only 2 monodentate carboxylates in all four structures, meaning that of 40 carboxylate O atoms only 2 are left uncoordinated; belonging to **I**-L3 and **III**-L2.

Despite the phase diversity, all tartrate binding to the Cd atoms is dominated by the '1,2-chelation' involving a carboxylate oxygen and its neighboring hydroxyl group. In fact, in all the structures only one carboxylate (tartrate **I**-L3, Scheme 1b) does not participate in this chelation. Here, the carboxylate is monodentate with the carboxylate O atom closest to the hydroxyl group left uncoordinated, imposing a steric constraint that prevents the formation of the 1,2-chelate ring. All the other tartrate ligands in structures **I**, **III** and **IV** have two 1,2-chelate rings, while in compound **II** they have one 1,2-chelate ring and a 1,2,3-tris chelate ring formed as a result of the μ_3-bridging alkoxide O atom. These 1,2-chelate rings are the essence of the dimeric units that build up many tartrate based compounds, including **III** and **IV**. By further inspection of the other structures presented in this work, a similar connectivity between pairs of Cd atoms was found. In the extended framework of compound **I**, a dimer is formed between Cd1 and its symmetrically equivalent Cd1′. In compound **II**, Cd1 and Cd2 are also connected by a similar dimer, which differs by the

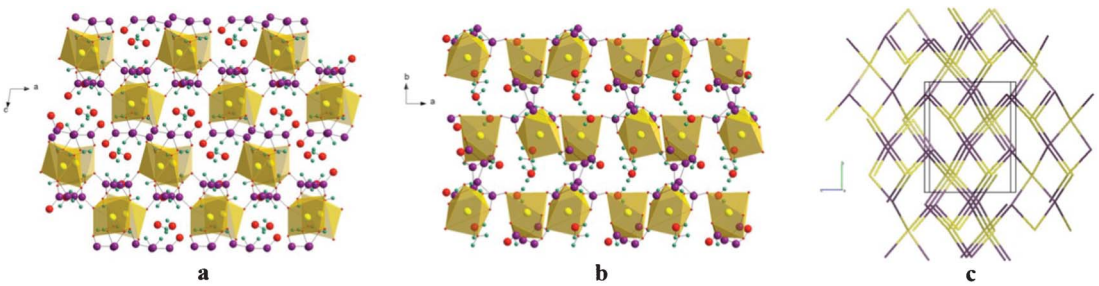

Fig. 7 (a) View of the extended structure of **III** along the crystallographic *b* axis and (b) *c* axis showing the framework channels pores. (c) Schematic representation of the network topology.

1,2,3-tris chelate rings involving the alkoxide O atom; also seen in other structures.[5,8]

Infrared spectroscopy

The IR spectra show a broad band in the region of 3507–2560 cm^{-1} for **I**, 3601–2505 cm^{-1} for **II**, 3490–2577 cm^{-1} for **III** and 3513–2433 cm^{-1} for **IV**. This band corresponds to the ν(OH) stretching modes of the water molecules (both coordinated and non-coordinated) and the OH groups in the tartrate chains; its broadening is caused by the hydrogen bonds between these molecules.

For all compounds, the absence of the absorption band around 1700 cm^{-1} confirms that the carboxylate groups in the tartrate ligands are completely deprotonated; their asymmetric ν_{as}(OCO) and symmetric ν_s(OCO) stretching vibrations are found in the region of 1600–1300 cm^{-1}. These bands are sensitive to the nature of the bonding with the metal ions; therefore, their separation is also indicative of the structure of a given carboxylate. Several rules have been established in the literature[41] to relate the coordination modes of the carboxylate groups with the separations between the bands ($\Delta\nu$). In compounds **I–IV** there is overlapping of the carboxylate stretching bands due to the multiple carboxylate groups present in each structure. For this reason, in general it was only possible to identify one delta for each coordination mode, rather than assign one delta to each carboxylate present in the structure (Table 3). These assignments are based on the results found by single crystal X-ray diffraction.

Thermal analysis and dehydration–hydration cycles

According to thermogravimetric experiments, the dehydration and decomposition processes of all compounds are clearly separated. This behavior suggests that after dehydration, open framework spaces should be available for other adsorbate molecules. The thermograms of compounds **I–III** revealed three thermal events (Fig. 8). The temperature, weight loss and assignment during the stages of dehydration and decomposition are presented in Table 4.

For all three samples, the first weight loss starts at room temperature and can be associated to the desorption of the lattice water molecules; the final temperature of this process depends on the crystal structure. The difference between the number of lattice water molecules estimated by TGA and X-ray diffraction is due to the desorption of some water molecules during the setup of the TG experiment; where the sample is exposed to an atmosphere of dry air for several minutes before the analysis starts. After the lattice water molecules evolve, a gradual weight loss occurs up to the onset temperatures for decomposition. The decomposition takes place in two stages, with a total weight loss corresponding to the evolution of the coordinated water molecules and tartrate ligands in the molecular formula obtained by single crystal X-ray diffraction.

Table 3 Assignment of coordination modes related to $\Delta\nu$ in **I–IV**

	$\Delta\nu$, cm^{-1}	Coordination mode of carboxylate groups
I	252	Monodentate
	165	Chelating–bridging tridentate
	142	Bridging bidentate
II	260	Chelating–bridging tridentate
	151	Bridging bidentate
III	204	Monodentate
	165	Bridging bidentate
IV	252	Bridging bidentate (attributed to the more distorted groups in L1)
	165	Bridging bidentate (attributed to the more symmetrical groups of L2 and L3)

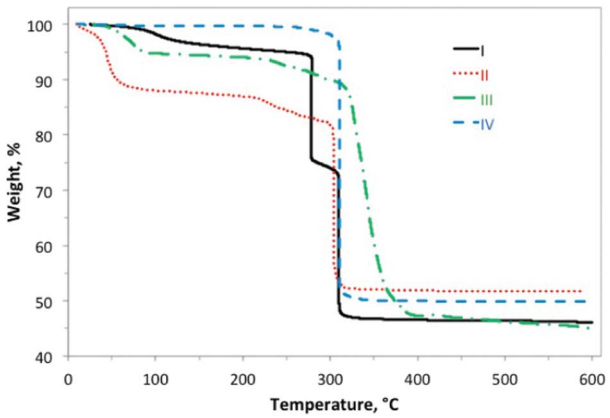

Fig. 8 High resolution thermogravimetric curves of **I–IV**.

The thermogram of compound **IV** only has one weight loss of 50.06% at 310 °C, which can be assigned to the evolution of one tartrate ligand (calculated weight loss: 50.70%). In this sample all lattice water molecules evolved during the setup of the experiment.

The reversibility of the dehydration process for compounds **I–III** was corroborated by three dehydration–rehydration cycles. Fig. 9 shows the profile of mass as a function of time for compound **I**; the profiles for **II** and **III** are similar. In all three cases, the mass loss and the corresponding weight loss in the thermogravimetric curves are comparable. The hydration profile of all three compounds revealed that 24 h were not enough to completely rehydrate the samples. For all three compounds, the X-ray powder diffraction patterns after the three cycles confirmed retention of crystallinity.

According to the pore sizes of the hydrated samples of compounds **II** and **III**, the channel dimensions are significantly

Table 4 TGA data[a] for **I–III**

	I	II	III
Dehydration			
T_{end}, °C	165	90	85
wl_{exp}, %	3.40	11.84	5.99
n	1.8	5.0	1.9
Decomposition			
T_o, °C	275	217	229
T_f, °C	310	304	391
wl_{exp}, %	49.76	36.19	48.53
wl_{cal}, %	49.83	37.25	49.22
Assignment	$(H_2O)(C_4H_4O_5)_3$	$(H_2O)_2(C_4H_3O_{4.5})_2$	$(H_2O)(C_4H_4O_5)_2$

[a] T_{end}: final temperature, wl_{exp}: experimental weight loss, n: corresponding number of water molecules per formula, T_o: extrapolated onset temperature, T_f: extrapolated final temperature, and wl_{cal}: calculated weight loss.

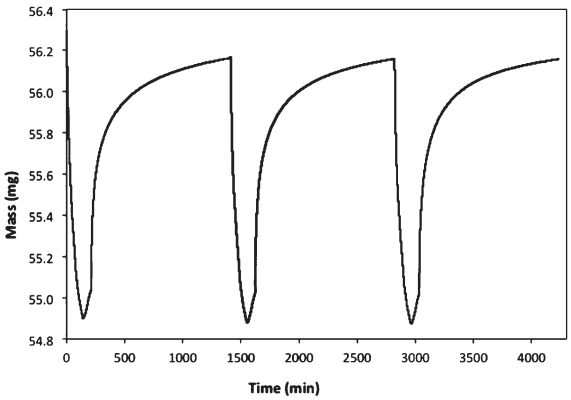

Fig. 9 Three dehydration–hydration cycles in compound **I**.

larger than the water molecule; additionally, the calculations with PLATON revealed 27.7% and 17.2% solvent-accessible void space respectively. Therefore, the possibility of flexible frameworks with pore dimensions dynamically modified by the adsorbed amount should not be discarded.

For compound **I**, no residual solvent-accessible void could be estimated by PLATON; however, since one lattice water molecule was removed from the CIF file to carry out the calculation, at least a low percentage of void space would be expected. In addition, this null estimation is inconsistent with the experimental results obtained by TGA and the dehydration–hydration cycles, both of which corroborate the reversibility of water diffusion in and out of the framework. Nonetheless, PLATON's result is likely an indication of small pores. According to the crystal structure description, the cavities containing the lattice water molecules are connected to narrow channels; this fact, added to the probable flexibility of the framework due to the tartrate ligands, could explain this apparent lack of void space.

Conclusions

In this paper, we successfully combined the merits of the tartrate ligand and Cd(II) atom to synthesize four coordination polymers with different architectures. Compounds **I–III** are structurally determined and reported here for the first time. A fourth compound (**IV**) already reported[2,24] was also reproduced under different synthetic conditions.

In all four compounds, the tartrate anion displays diversiform bridging fashions in the structural assembly, where the hydroxyl groups (protonated and deprotonated) always participate in the bonding. The ligands of compounds **I**, **III** and **IV** have similar coordination modes, which vary significantly from compound **II** owing to the presence of a deprotonated hydroxyl group. The 1,2-chelate rings, formed between a hydroxyl group and its neighboring carboxylic group, represent a characteristic interaction mode of the tartrate ligand. They are the essence of the dimeric units that build up many tartrate-based compounds, including **III** and **IV**; and they are present in the extended framework of compounds **I** and **II**.

The assemblies of compounds **I–IV** all gave rise to open frameworks. Compound **IV** has an anhydrous framework, while compounds **I–III** have coordinated water molecules that could be removed upon dehydration to leave unsaturated metal sites, making them potentially useful for gas adsorption and catalysis. The size of the framework pores in compound **II** makes it particularly interesting for applications in gas storage and separation. As opposed to the other compounds studied here, some of its pores are built up entirely by the inorganic unit; therefore they are more rigid than those affected by ligand flexibility.

Acknowledgements

This research was partially supported by the Projects: SEP–CONACYT-154626, DGAPA-IN-102512, CONACYT-SENER-117373, CONACYT-CB2007-82964. The authors thank E. Fregoso, S. López, K. Díaz and G. Cedillo for their technical assistance. Thanks are given to the Consejo Superior de Investigaciones Científicas (CSIC) of Spain for the award of a license for the use of the Cambridge Crystallographic Data Base (CSD).

References

1 Z. Derewenda, *Acta Crystallogr., Sect. A: Found. Crystallogr.*, 2007, **64**, 246–258.
2 (*a*) J. Lu, H.-T. Liu, D.-Q. Wang, M.-J. Niu and S.-N. Wang, *J. Chem. Crystallogr.*, 2011, **41**, 641–648; (*b*) L.-Z. Zhao, P. Li, B.-L. Cao and S. W. Ng, *Acta Crystallogr., Sect. E: Struct. Rep. Online*, 2009, **65**, m629.
3 K. C. Kam, K. L. M. Young and A. K. Cheetham, *Cryst. Growth Des.*, 2007, **7**, 1522–1532.
4 Y. Wang, G.-X. Liu, Y.-C. Chen, K.-B. Wang and S.-G. Meng, *Inorg. Chim. Acta*, 2010, **363**, 2668–2672.
5 A. S.-F. Au-Yeung, H. H.-Y. Sung, J. A. K. Cha, A. W.-H. Siu, S. S.-Y. Chui and I. D. Williams, *Inorg. Chem. Commun.*, 2006, **9**, 507–511.
6 P. Schwendt, P. Svancarek, L. Luchta and J. Marek, *Polyhedron*, 1998, **17**, 2161–2166.
7 S. Kaizaki, M. Urade, A. Fuyuhiro and Y. Abe, *Inorg. Chim. Acta*, 2006, **359**, 374–378.
8 H. Yao, M. Ji, S. Ji, Y. Jiang, L. Li and Y. An, *Inorg. Chem. Commun.*, 2007, **10**, 440–442.
9 J. A. Rood, B. C. Noll and K. W. Henderson, *J. Solid State Chem.*, 2010, **183**, 270–276.
10 C. Ge, Z. Zhao, G. Han and X. Zhang, *Acta Crystallogr., Sect. E: Struct. Rep. Online*, 2008, **64**, m360.
11 D.-X. Li, D.-J. Xu and Y.-Z. Xu, *Acta Crystallogr., Sect. E: Struct. Rep. Online*, 2004, **60**, m1982.
12 F. Salles, G. Maurin, C. Serre, P. L. Llewellyn, C. Knöfel, H. J. Choi, Y. Filinchuk, L. Oliviero, A. Vimont, J. R. Long and G. Férey, *J. Am. Chem. Soc.*, 2010, **132**, 13782–13788.
13 H. J. Park and M. P. Suh, *Chem.–Eur. J.*, 2008, **14**, 8812–8821.
14 S. Henke, F. D. C. Wieland, M. Meilikhov, M. Paulus, C. Sternemann, K. Yusenko and R. A. Fischer, *CrystEngComm*, 2011, **13**, 6399–6404.
15 D. N. Dybtsev, H. Chun and K. Kim, *Angew. Chem., Int. Ed.*, 2004, **43**, 5033–5036.
16 S. P. Anthony, C. Delaney, S. Varughese, L. Wang and S. M. Draper, *CrystEngComm*, 2011, **13**, 6706–6711.
17 E. Coronado, J. R. Galán-Mascarós, C. J. Gómez-García and A. Murcia-Martínez, *Chem.–Eur. J.*, 2006, **12**, 3484–3492.
18 I. Imaz, M. Rubio-Martínez, J. An, I. Solé-Font, N. L. Rosi and D. Maspoch, *Chem. Commun.*, 2011, **47**, 7287–7302.
19 P. L. Llewellyn, P. Horcajada, G. Maurin, T. Devic, N. Rosenbach, S. Bourrelly, C. Serre, D. Vincent, S. Loera-Serna, Y. Filinchuk and G. Férey, *J. Am. Chem. Soc.*, 2009, **131**, 13002–13008.
20 S. Mondal, M. Mukherjee, S. Chakraborty and A. K. Mukherjee, *Cryst. Growth Des.*, 2006, **6**, 940–945.
21 R. Zou, A. I. Abdel-Fattah, H. Xu, Y. Zhao and D. D. Hickmott, *CrystEngComm*, 2010, **12**, 1337–1353.

22 E. V. Brusau, J. C. Pedregosa, G. E. Narda, G. Pozzi, G. Echeverria and G. Punte, *J. Coord. Chem.*, 2001, **54**, 469–480.
23 M. Tabatabaee, A. Gholamighavamabad, E. Khabiri and M. Parvez, *J. Inorg. Organomet. Polym. Mater.*, 2011, **21**, 627–633.
24 L.-Z. Zhao, P. Li, B.-L. Cao and S. W. Ng, *Acta Crystallogr., Sect. E: Struct. Rep. Online*, 2009, **65**, m629.
25 C. González-Silgo, J. González-Platas, C. Ruiz-Pérez, T. López and M. E. Torres, *Acta Crystallogr., Sect. C: Cryst. Struct. Commun.*, 1999, **55**, 710–712.
26 M. E. Torres, T. López, J. Peraza, J. Stockel, A. C. Yanes, C. González-Silgo, C. Ruiz-Pérez and P. A. Lorenzo-Luis, *J. Appl. Phys.*, 1998, **84**, 5729–5732.
27 G. M. Sheldrick, *A Program for the Siemens Area Detector Absorption Correction*, Göttingen, Germany, 2008.
28 G. M. Sheldrick, *Acta Crystallogr., Sect. A: Found. Crystallogr.*, 2008, **64**, 112–122.
29 P. van der Sluis and A. L. Spek, *Acta Crystallogr., Sect. A: Found. Crystallogr.*, 1990, **46**, 194–201.
30 A. L. Spek, *Acta Crystallogr., Sect. D: Biol. Crystallogr.*, 2009, **65**, 148–155.
31 V. A. Blatov in *IUCr CompComm Newsletter,*, TOPOS is available at http://www.topos.ssu.samara.ru, 2006, **7**, pp. 4–38.
32 Y. Matsumoto, E. Miki, K. Mizumachi, T. Ishimori, T. Kimura and T. Sakurai, *Chem. Lett.*, 1981, 1401–1404.
33 L. J. Bostelaar, R. A. G. de Graaff, F. B. Hulsbergen, J. Reedijk and W. M. H. Sachtler, *Inorg. Chem.*, 1984, **23**, 2294–2297.
34 H.-T. Liu, J. Lu and D.-Q. Wang, *Acta Crystallogr., Sect. E: Struct. Rep. Online*, 2010, **66**, m374.
35 S. Scherb, C. Näther and W. Bensch, *Acta Crystallogr., Sect. C: Cryst. Struct. Commun.*, 2002, **58**, m135–m136.
36 L. K. Templeton, D. H. Templeton, D. Zhang and A. Zalkin, *Acta Crystallogr., Sect. C: Cryst. Struct. Commun.*, 1985, **41**, 363–365.
37 D. Bayot, B. Tinant and M. Devillers, *Inorg. Chem.*, 2005, **44**, 1554–1562.
38 M. Nakahanada, T. Fujihara, N. Koine and S. Kaizaki, *J. Chem. Soc., Dalton Trans.*, 1992, 3423–3426.
39 C. K. Prout, J. R. Carruthers and F. J. Rossotti, *J. Chem. Soc. A*, 1971, 3336–3342.
40 C. Ruiz-Pérez, M. Hernández-Molina, C. González-Silgo, T. López, C. Yanes and X. Solans, *Acta Crystallogr., Sect. C: Cryst. Struct. Commun.*, 1996, **52**, 2473–2475.
41 G. B. Deacon and R. J. Phillips, *Coord. Chem. Rev.*, 1980, **33**, 227–250.